Investigation of Process Parameters in High-Speed Die-less Water Jet Spin-Forming of Copper Sheets

Mehrdad Asadi
Islamic Azad University Khomeini Shahr Branch
Mohsen Loh-Mousavi (loh-mousavi@iaukhsh.ac.ir)
Islamic Azad University Khomeini Shahr Branch https://orcid.org/0000-0001-5108-5663
Ali Heidari
Islamic Azad University Khomeini Shahr Branch
Kamran Amini
Islamic Azad University

Research Article

Keywords: High speed, Water jet spin-forming, Copper sheets, Sheet forming, Surface quality

Posted Date: September 3rd, 2021

DOI: https://doi.org/10.21203/rs.3.rs-848145/v1

Abstract

A new forming method called high speed water jet spin-forming was developed. This new forming method is a combination of water jet incremental forming and sheet metal spinning without any mandrel. The forming speed has been significantly increased by spinning of the sheet using a lathe machine. The effects of the forming parameters such as water jet pressure, rotation speed and relative water jet diameter on formability and surface quality of deformed copper parts were investigated. The experimental results indicate that the water jet pressure and the sheet rotation speed have a significant effect on the final depth, wall angle, and surface smoothness. It was also concluded that the final depth exponentially increases as the sheet rotational speed reduced. In addition, when the water jet pressure is low, sheet rational speed does not play a significant role in the final depth of the specimen. Furthermore, it has been determined from the results that high water jet pressure plays an important role in improving the surface quality and wrinkling at different rotational speeds, and as the pressure is increased, the wrinkling decreases and thus the surface quality is improved.

1. Introduction

Nowadays, water jet technology has been utilized in various manufacturing processes due to its numerous advantages that can be used for sheet forming processes as well as cutting, blasting, and peening [1–2]. Water jet spot welding is one of the applications of water jet technology to create a high speed joint between metallic surfaces [3–4].

Water jet incremental forming (WJIF) is one of the relatively new sheet metal forming processes, which has many advantages such as flexibility, surface smoothness, environmental compatibility, and low cost of equipment. However, this forming method has a limitation of long forming time compared to conventional incremental sheet forming (ISF) [5]. On the other hand, sheet metal spinning is a faster sheet metal forming process compared to ISF; therefore, a combination of spinning with WJIF can increase the speed of forming. This new process is introduced as water jet spin forming (WJSF). In the sheet metal spinning process, a mandrel or die is usually used to support the sheet whereas die-less water jet spin forming can be performed without any die or mandrel similar to the incremental forming process. In this process, a sheet is placed and clamped in a holder which is composed of two pieces as shown in Fig. 1. The holder is placed inside a three-jaw chuck of a lathe machine and it is rotated at a constant speed. The water jet (WJ) nozzle is fixed on the tool post of the lathe machine in a manner that allows transverse motion. The nozzle is positioned at a specific distance from the sheet and continuously moves toward the center during the rotation of the sheet at a constant speed.

Jurisevic et al. investigated the basic simulation principles of WJIF based on a combination of computational fluid dynamics (CFD) and finite element method (FEM) [5]. In addition, they compared the advantages and disadvantages of the WJIF and ISF. It was shown that the higher forming speed, accuracy, and energy efficiency are the main disadvantages of the WJIF process. Iseki utilized WJ as a forming tool to produce various complex aluminium shapes with a speed of 5 mm/s. The deformation of the aluminium sheet was analysed by a plane strain theory and it is concluded that the WJ can be used instead of the rigid tools to form the sheets [6]. Jurisevic et al. illustrated the pressure and velocity profiles of WJ using two-dimensional finite-element simulation [7–8]. In addition, they introduced laminated supporting tools to increase the accuracy of the WJIF process. Comparisons between four different forming trajectories were performed to reduce the forming time and improve the product quality in which the minimum forming time was about 5.53 min [9]. The comparison between the parameters of the WJ cutting process and the WJ forming process was performed by Junkar et al. [10]

Several researchers have compared the deformation behaviour during WJ tube forming by experiments and numerical simulations [11–12]. Teymoori et al. simulated the WJIF process based on an Eulerian-Lagrangian approach by a three-dimensional simulation. The forming process was performed in the form of concentric circles at a speed of 2.5 mm/s. In addition, several parameters such as final deformation and thickness distributions of the deformed parts were investigated [13].

Tokuhiro et al. proposed a die-less shear spinning using multipurpose elastomers instead of using rigid mandrels [14]. They formed a double-curved part of an aircraft by using this technique with a rotation speed of 120 RPM [15]. The utilization of oil instead of water as a forming tool was studied by Zhang et al. to increase the deformation depth [16]. The effect of the nozzle geometry on the velocity and pressure was investigated by theoretical analysis and numerical simulation. They also investigated the local bulging deformation of an aluminium sheet with a thickness of 0.3 mm by experimental and numerical methods.

He et al. evaluated the effects of the forming parameters such as water jet pressure and feeding speed [17]. Li et al. presented a theoretical model based on the plane strain model to study a die-less WJIF [18]. They studied the relation between the key parameters for WJ pressure and the forming angle of a truncated cone. Yi Shi et al. investigated the effect of several parameters such as WJ pressure, relative WJ diameter, and feed rate. The application of WJ incremental micro-forming (WJIMF) processes were introduced by She et al. using experimental methods and simulations [19–20]. The results of these experiments and simulations showed that WJ pressure is a vital parameter in WJIMF and thus increasing WJ pressure increases the wall angle linearly. In addition, some effects of different process parameters such as nozzle diameter and pressure on the wall angle and surface smoothness in WJIF were investigated experimentally. Yi Shi et al. proposed WJIMF with a supporting die to produce complex parts using the WJIF method. The final depth is not well controlled due to the effect of several parameters. To solve this problem, the application of several kinds of supporting dies was studied. They also reported that the tool path could affect the forming accuracy [21].

Zhang et al. studied the local bulging of 50-micron thin copper foil by WJIF to evaluate the parameters such as WJ pressure and nozzle distance numerically and experimentally. To simulate the interaction of the WJ with the sheet, the fluid-solid coupled method was utilized [22]. A new ISF-WJ prototype machine was proposed to combine WJIF and ISF with rigid tool processes at a speed of 50 RPM by Lu et al. [23]. Four nozzles with the same inlet and outlet diameters and different internal geometries were simulated to obtain the maximum pressure. To obtain the appropriate nozzle, the CFD simulation was carried out by the ANSYS/Fluent software. It was found that WJ pressure played an important role in the WJIF process. As mentioned in the literature of this study, the previous research works on WJIF have mostly focused on the laboratory scale or micro-size (small scale) and just a few papers can be found about WJ forming of real industrial-scale parts.

This paper focuses on the key parameters in the water jet spin forming process of medium-scale copper parts. To achieve this goal, several forming parameters such as sheet rotation speed and WJ pressure have been investigated experimentally by an innovative method. The WJSF process has been performed at speed of 1000 RPM using this new technique which can produce full cone shapes with industrial size by the proposed industrial set-up. The prediction of the yield and the final working pressure for the WSJF process is also presented to obtain the technological process window. Moreover, the effects of the WJ pressure and rotational speed on cross-sectional shapes of the deformed area, final depth, wall angle, and surface quality of the formed sheets are studied.

2. Experimental Procedure

The proposed setup to perform WJSF is shown in Fig. 2. The setup includes a lathe machine, a three-phase motor, a piston pump, a pressure gauge, a WJ nozzle, and a holder.

A piston pump was used in this process and it provided the maximum flow rate and pressure of 48 lit/min and 40 MPa, respectively. The maximum electrical power of the electric motor was 20 HP to provide this flow and pressure. Fig 3. shows the piston pump with the pressure control valve, discharge control, pressure gauge, and three-phase electric motor.

The holder is composed of top and bottom pieces. The sheet is clamped between the holder and the holder is placed inside the three-jaw chuck which can rotate the sheet at a speed between 22 to 1000 RPM. In addition, the water-jet nozzle is positioned on the lathe machine in a manner that allows transverse motion. The nozzle is placed at a specific distance from the sheet and continuously moves toward the center during the rotation of the sheet with a constant feed rate as shown in Fig. 4.

The developed industrial WJSF was a combination of WJIF and sheet metal spinning, which significantly reduces the forming time due to the high rotational speed. Moreover, the final surface quality may be improved by the rotational speed of the sheet. The forming time was less than 6 (s) at the rotational speed of 1000 RPM which is very lower than regular water jet incremental forming.

The water was splashed from the nozzle at high pressure as the three-jaw chuck is turned at the same time. Meanwhile, the metal sheet rotates on the chuck and the nozzle gradually advanced toward the center where the forming process ends. According to this relative movement of nozzle and sheet, as shown in Fig. 5 a spiral WJ path is defined that leads to a cone-shaped part. The final shapes of the specimens are complete cones with a diameter of 80 mm; however, deforming the sheets with different parameters and without any die or mandrel leads to different final depth.

Soft pure copper sheets (Cu-ETP) with different thicknesses of 0.1, 0.15, and 0.2 mm and the same diameter of 120 mm were utilized in the experiments. The mechanical properties of the copper sheet are shown in Table 1.

Table 1 Mechanical properties of copper (Cu-ETP) sheet and effective process parameters used in experimental

Parameter	Value
Density (kg/m^3)	8800
Young's modulus (GPa)	117
Yield stress (MPa)	90
Ultimate stress (MPa)	237
Poisson's ratio (-)	0.34
Strength coefficient (K) (MPa)	383
Strain-hardening exponent (n) (-)	0.32
Sheet thickness (mm)	0.1, 0.15 ,0.2
Rotational speed of sheets (RPM)	1000, 500, 90, 22
Feed rate (mm/rev)	0.8
Water pressure (P_W)	2, 4, 5, 6, 8, 10.5, 28
Stand-off distance (h_{SO}) (mm)	30
Nozzle discharge coefficient (C_D)	0.8
Nozzle Diameter (mm)	1.25

The effective process parameters are described as the water pressure at nozzle inlet (P_W), the initial distance between the sheet metal and the nozzle outlet (h_{SO}), nozzle travel velocity or rotational of the sheet (v_T), the nozzle outlet diameter (d_{WJ}), and the nozzle discharge coefficient (C_D).

3. Results And Discussion

3.1. Technological window of WJSF for different thicknesses

Yield pressure and final pressure are the most effective parameters in sheet metal forming processes. The yield pressure is a pressure that causes plastic deformation in sheet metal and the final pressure is a pressure that brings the sheet about tearing during the forming. The yield and final working pressures are specified to select the pressure parameters to evaluate the effect of pressure on WJIF. Therefore, the yield pressure and final pressure for the copper sheets of 0.1, 0.15, and 0.2 mm thickness with the same forming conditions in Table.1, and the rotary velocity (VT) of 1000 RPM were examined experimentally. The formed specimens to obtain the yield pressure and final pressure with thicknesses of 0.1 and 0.2 are shown in Fig. 6.

As it can be seen from Fig. 6 there are several wrinkles on the specimens that were formed by the low pressure around the yield pressure whereas there are no wrinkles for those specimens that were formed with high pressure near to the final pressure. Therefore, the quality of the final surface increases by increasing the forming pressures. The results of the experiments to specify the yield pressure, final pressure, obtained final depths, and wall angles for the different sheet thicknesses are given in Table 2.

Table. 2 Yield pressure, final pressure, final depth, and wall angle for different sheet thicknesses

Parameters	**Value**		
Initial thickness (mm)	0.1	0.15	0.2
Yield pressure (MPa)	2	3.4	5
Final depth for yield pressure (mm)	2.7	3.4	3.1
Final pressure (MPa)	10.5	19	28
Final depth for final pressure (mm)	38.3	38.6	39.1
Wall angle for yield pressure (q)	3.86	4.86	4.43
Wall angle for final pressure (q)	43.76	43.98	44.35

The relation between the sheet thickness and WJ pressure for the three different thicknesses of the copper sheet was experimentally examined. It can be found from the table that the final depth and the wall angle for the yield pressure and final pressure of the sheets are approximately equal with thicknesses of 0.1, 0.15, and 0.2 mm. It is clear that as the sheet thickness increases, the yield pressure and final pressure also are increased. Therefore, by increasing pressure at each thickness; the final depth and wall angle also are increased.

The relation between relative jet diameter (Ϗ) and WJ pressure for the three different sheet thicknesses was also investigated. The relative jet diameter (Ϗ) is a non-dimensional parameter that depends on the WJ diameter and the initial thickness of the sheet (t_0) as defined in Eq.(1) which was extracted by Jurisevic et al. [5].

$$\text{Ϗ}= \frac{d_{WJ}}{t_0} \qquad (1)$$

Ϗ was calculated using Eq. (1) for each thickness as shown in Table. 3. It can be found that, for the lowest initial thickness of the sheet, Ϗ is the highest value and the Ϗ decreased with increasing sheet thickness. On the other hand, when the initial thickness is low, the difference between the yield pressure and the final pressure is low, and as the thickness increases, the pressure difference increases.

Table. 3 The calculated relative jet diameter (Ϗ) for different thicknesses

Initial thickness (mm)	Ϗ	Yield pressure (MPa)	Final pressure (MPa)
0.1	12.5	2	10.5
0.15	8.33	3.4	19
0.2	6.25	5	28

As it is mentioned by Jurisevic et al. [5] a technological window can be presented to obtain process parameters as shown in Fig. 7, which is a schematic diagram of this process. This diagram is one of the important typical diagrams in designing the process of WJIF that is based on two parameters, Ϗ and WJ pressure (P_W).

The upper area of the technological window is limited by the erosion starting line, and the lower area of the technological window is limited by the yield start curve as shown in Fig. 7. In this research, the technological window of this process is obtained experimentally that composed of three parts and separated by two curved lines. Below the bottom line is the area where plastic deformation doesn't occur on the sheet. Between the bottom curve and the top line is the technological window area for WJS process which forming process is completely performed in this area.

Fig. 8 shows the obtained experimental technological window of WJSF of different thicknesses. In this diagram, the lower bound shows the yield pressure boundary, and the upper bound shows the boundary margin of tear pressure of the sheet with different thicknesses. There are two values for each K_i, one for the minimum pressure (yield pressure) and the other for the maximum pressure (final pressure) that can be seen on the bottom and top lines, respectively. The intermediate region between the lower bound and the upper bound is a technological process window to perform a successful forming by WJSF. It can be seen, the variation of the boundary curve of yield pressure is less than that for the tearing boundary curve while the variations of both curves become constant for the larger relative jet values.

In the proposed schematic diagram by Jurisevic et al. [5], a tearing boundary was not presented in the technological window and only the erosion boundary was illustrated, while in the obtained graph in this research, tearing boundary is presented.

3.2. Effect of water jet pressure at different rotational speed on deformation

WJ pressure is one of the effective parameters in the WJIF process. Therefore, the WJ pressure parameter for three different rotational speeds of sheets was investigated. To perform this study, the parameters of WJ pressure and sheet rotation speed were examined. Thus, different water jet pressures of 4, 6, and 8 MPa were initially examined with a constant rotary speed. Subsequently, the same pressures were re-examined after changing the rotary speed for the other specimens. The deformed parts using WJSF with rotational speeds of 1000 RPM, 90 RPM, and 22 RPM for copper sheets with a thickness of 0.1 mm with different pressures are illustrated in Figs. 9, 10, 11.

The specimens which formed using a rotational speed of 1000 RPM with the pressures of 4, 6, and 8 MPa were not formed appropriately and several wrinkles can be observed on the deformed parts. It can be concluded that as the WJ pressure increases, the wrinkles in the parts decrease. The forming time was about 6 seconds for the speed of 1000 RPM.

As shown in Fig. 10, three other experiments have been carried out at a speed of 90 RPM for the same pressures of 4, 6, and 8 MPa to investigate the effect of WJ pressure during the WJSF process. As it can be seen from the figure, several small grooves were formed on the deformed parts. The forming time for the speed of 90 RPM was about 66 seconds. It can be found that, while WJ pressure is high, despite the reduction in the forming time, the quality of the formed sheet and also surface roughness is improved.

As shown in Fig. 11, three specimens were formed with a rotational speed of 22 RPM and WJ pressures of 4, 6, and 8 MPa. Unlike previous speeds where several wrinkles and grooves were formed on the specimens, no wrinkle or groove occurred on the specimens using a rotational speed of 22 RPM with different WJ pressures. It is mentioned that the forming time was about 273 seconds for this rotational speed.

Focusing on Fig. 9 and Fig. 10 reveals an interesting phenomenon which is the effect of pressure on orientations of wrinkles and grooves. It can be seen that in Figs (9-a) and (9-c) wrinkles are clockwise and in Fig. (9-b) the wrinkles have no orientation and several radial wrinkles can be seen. Similarly, the orientation of the grooves in Fig. (10-a) is clockwise and in Fig. (10-b) is radial, whereas grooves in Fig. (10-c) are counter-clockwise.

3.3. Effect of water jet pressure on final depth and cross-sectional shape

The final depths of the deformed parts with the rotational speed of 22, 90, and 1000 RPM for the pressures of 4, 6, and 8 MPa are shown in Fig. 12. The final depth obtained using the WJ pressure of 4 MPa is approximately equal at all three speeds of 1000, 90, and 22 RPM. Although the speed of 22 RPM slightly increased the final depth, the speed of 1000 RPM led to the lowest final depth in the formed specimens.

It is clear that for all three speeds the final depth obtained by the pressure of 6 MPa is greater than for the pressure of 4 MPa whereas the effect of the rotational speed on final depth at pressures of 6 and 8 MPa is greater than that of the pressure of 4 MPa. It is observed that with increasing WJ pressure the effect of the rotational speed on the final depth increases. At the beginning of the forming, the rotational speed does not have large effect on the deformation, whereas as the plastic area develops and the forming time becomes longer, the rate of plastic deformation increases.

The cross-sectional shapes of the deformed parts with a rotational speed of 1000 RPM for different pressures are illustrated in Fig. 13. As can be seen, the final depths of the deformed specimens are different and it indicates the increase of pressure proportionally increases the depth of the deformed part.

The specimens formed using a speed of 1000 RPM with pressures of 4 and 8 MPa have a final depth of 14.3 and 24.7 mm, respectively, so with an increase in pressure of 4 MPa, the final depth is 10.4 mm increased. The specimens formed using a speed of 90 RPM with pressures of 4 and 8 MPa have a final depth of 14.9 and 33.8 mm, respectively, so with an increase in pressure of 4 MPa, the final depth is 18.9 mm increased. The specimens formed using a speed of 22 RPM with pressures of 4 and 8 MPa have a final depth of 15.8 and 39.1 mm, respectively, so with an increase in pressure of 4 MPa, the final depth is 23.3 mm increased.

3.4. Effect of rotational speed on deformation and depth

Nozzle displacement speed or sheet rotation is another effective parameter in this process. Fig.14 illustrates the formed specimens using a pressure of 8 MPa and different rotational speeds for copper sheets with a thickness of 0.1 mm. The rotation speed of the sheet was the only changing parameter in this section that varied from 22 to 1000, so the other effective parameters in this process were constant.

The WJSF process was performed with each speed of 1000, 500, 90, and 22 RPM. The forming time for each of the mentioned speeds was about 6, 12, 66, and 273 seconds, respectively.

As can be seen from Fig. 14, for the speed of 1000 RPM, relatively large wrinkles have occurred on the specimen while for the speeds of 500 and 90 RPM, many small grooves or waviness appeared. The surface smoothness of the specimen, which is formed at a speed of 22 RPM, looks excellent because it is free of any wave or groove. Fig. 15, shows the final depth of the specimens formed at different speeds for the WJ pressure of 8 MPa. As the sheet rotation speed increases, the final depth decreases and more importantly, the final depth increases exponentially.

The specimens were formed using the speeds of 22 and 1000 RPM and pressures of 8 MPa have a final depth of 39.1 and 24.7, respectively. Thus, by reducing the speed from 1000 to 22 RPM, the final depth increases about 14.4 mm.

3.5. Effect of water jet pressure and rotational speed of sheet on wall angle

The wall angle is also one of the important results in investigation of deformed cone specimens. To evaluate the effect of the parameters on the cone specimens, this output was studied. Based on the final depth of the specimens in the previous sections, the wall angle was obtained. Fig. 16 shows the measured wall angles for pressures of 4, 6, and 8 MPa and speeds of 22, 90, and 1000 RPM. The results indicate, as the pressure increases, the wall angle of the specimens’ increases linearly.

It is also can be seen from the figure that a slight difference between the wall angles of specimens formed using speeds of 1000 RPM and with pressures of 4 and 8 MPa, whereas a large difference between the wall angles of specimens formed at speeds of 22 at pressures 4 and 8 can be observed.

On the other hand, at the pressures of 4 MPa, for speeds of 22, 90, and 1000 RPM, the wall angles of the specimens are very close to each other. At the pressures of 6 and 8 MPa, the differences between the wall angles of the specimens are greater than that for the pressures of 4 MPa.

The wall angles of the deformed specimens with the pressure of 8 MPa for different sheet rotation speeds of 22, 90, 500, and 1000 RPM are compared in Fig. 17. It can be seen that by increasing the rotation speeds of the sheets, the wall angles are reduced. The wall angles of the formed specimens by pressure of 8 MPa and speeds of 22, 90, 500, and 1000 are about 44.35, 40.19, 34.7, and 31.68, degrees respectively. The lowest wall angle is related to the formed specimen with a speed of 1000 RPM and the maximum wall angle is related to the rotation speed of 22 RPM. The difference between the minimum and maximum wall angles is about 12.67 degrees.

3.6. Effect of rotational speed and WJ pressure on surface quality

The effect of WJ pressure and rotational speed on surface roughness, waviness and grooves of deformed parts were investigated. The maximum surface roughness of the deformed parts with the rotational speed of 22, 90, and 1000 RPM for the pressures of 4, 6, and 8 MPa were measured by a digital roughness tester. The maximum roughness depth (Rmax) is the largest roughness depth within the evaluated specimens to evaluate the surface quality. The next three figures (18-20) show the surface roughness of the specimens formed at different speeds for the WJ pressure of 4, 6 and 8 MPa respectively. As can be seen from these figures, with increasing the rotational speeds of sheets, the maximum surface roughness has been increased.

In addition, to perform a qualitative surface investigation, several macroscopic photographs with different magnifications were prepared and compared. The macroscopic images for different pressures and rotational speeds are shown in Figs. 21 to 23.

Fig. 21 shows that the deformed specimens with the speed of 1000 RPM by different pressures have a few large wrinkles. The wrinkles formed on the specimens started from the centre of the cone and reaches to the outer area of the deformed area by the water jet.

Microscopic images of the formed specimens using a speed of 90 RPM and pressures of 4, 6, and 8 MPa are shown in Fig. 22. It is obvious that the many small wrinkles were formed at this speed and these small wrinkling lead the medium size grooves with different directions and paths on the deformed surfaces. Wrinkles in a specimen formed at a pressure of 4 MPa appear to be slightly smaller than those specimens formed at a pressure of 6 and 8 MPa.

Fig. 23 shows the microscopic images using a speed of 22 RPM and pressures of 4, 6, and 8 MPa. It is interesting that the deformed specimens with a speed of 22 RPM at all pressures have a better surface quality without any wrinkles or grooves. It means that, the wrinkles and grooves were decreased and even disappeared by the reduction of rotational speed of the rotating sheet during the process of WJSF.

To evaluate the effect of rotational speed on surface quality, two rotational speeds of 1000 and 22 RPM at the pressure of 4 MPa were selected and the required images were obtained using a scanning electron microscope (SEM) by the magnification of 50x. These two results are shown in Fig. 24 and it is illustrated that, there is a wrinkle on the formed specimen using the speed of 1000 RPM whereas there is not any surface defect or waviness on the formed specimen by the speed of 22 RPM and a very smooth and uniform surface occurred at the low speed of sheet rotation during the forming process.

4. Conclusions

In this paper, the effect of sheet rotational speed and WJ pressure on the high-speed water jet spin forming was investigated. An industrial set-up was developed to form conical copper parts using WJSF by supporting a lathe machine and this experimental set-up were successfully employed to find the following results:

1. Generally, the rotation speed should be decreased in the low pressure WJSF due to the possibility of wrinkles. The sheet rotational speed at low pressures does not change the final depth, whereas at high pressures, the reduction of rotational speed plays an important role in the increase of the final depth.
2. It was found that high water jet pressure plays an important role in reducing the wrinkles on the surface of deformed parts at different rotational speeds.

3. As the water jet pressure is increased, the wall angle of deformed part increases linearly while as the rotation speed of the sheet is increased the wall angle of deformed part decreases.
4. The experimental investigation of process parameters in the water Jet spin-forming of was performed to define the technological process window of WJSF of copper sheets.
5. The surface roughness and quality of the deformed parts are sensitive to the rotational speeds and WJ pressures. The surface quality decreases when the sheet rotational speed is increased.
6. Lathe machines are useful in increasing the forming speed of WJSF and to form industrial symmetrical metal parts by this forming process. The forming time was reduced at high-speed rotational speed of water jet spinning significantly compared to regular water jet incremental forming process.

Declarations

Ethics approval The manuscript contains original ideas which have never been published before in other journals. **Consent to participate** Not applicable

Consent for publication Not applicable

Conflict of interest The authors declare no competing interests.

References

1. Bañon F, Sambruno A, González-Rovira L, Vazquez-Martinez J M, Salguero J (2021) A review on the abrasive water-jet machining of metal–carbon fiber hybrid materials. Metals 11(1): 164

2. He Z, Zhao S, Ting F, Chen L, Zhang Y, Zhang M,Wang P (2018) Experimental and numerical analysis of water jet peening on 6061 aluminum alloy. J Press Vessel Technol 140(2): 021406

3. Ansari M A, Behnagh R A, Salvadori A (2021) Numerical analysis of high-speed water jet spot welding using the arbitrary Lagrangian-Eulerian (ALE) method. The Int J Adv Manuf Technol 112(1): 491-504

4. Chizari M, Al-Hassani STS, Barrett LM (2008) Experimental and numerical study of water jet spot welding. JMater Process Technol 198(1-3):213–219

5. Jurisevic B, Kuzman K, Junkar M (2006) Water jetting technology: an alternative in incremental sheet metal forming. The Int J Adv Manuf Technol 31:18–23

6. Iseki H (2001) Flexible and incremental bulging of sheet metal using high-speed water jet. JSME Int J Series C 44(2):468–493

7. Jurisevic B, Sajn V, Kosel F, Junkar M (2005) Experimental and numerical study of the tool in water jet incremental sheet metal forming. Proc 6th International Conference on Integrated Design in Mechanical Engineering, 11 pages

8. Sajn V, Jurisevic B, Kosel F (2011) Water jet incremental sheet metal forming: pressure distribution analysis. Int J Interact Des Manuf 5:95–102

9. Jurisevic B, Sajn V, Kosel F (2008) Introduction of laminated supporting tools in water jet incremental sheet metal forming. Int J Adv Manuf Technol 37:496–503

10. Junkar M, Heiniger KC, Jurisevic B (2004) Application of water jet technology for incremental sheet metal forming. J Mech Eng 50(12):613–622

11. Loh-Mousavi M, Teymoori F, Etesam A (2010) 3-D finite element simulation of water jet tube forming process. STEEL RESEARCH INTERNATIONAL, 81(9): 1466-1469

12. Chizari M, Barrett L M, Al-Hassani STS (2009) An explicit numerical modelling of the water jet tube forming. Computational Materials Science, 45(2): 378-384

13. Teymoori F, LohMousavi M, Etesam A (2016) Numerical analysis of fluid structure interaction in water jet incremental sheet forming process using coupled Eulerian–Lagrangian approach. Int J Interac Des Manuf 10(2):203–210

14. Tokuhiro S, Suzuki N, Takeuchi O (2018) Cylinder forming by die-less shear spinning with sheet thickness controlling of its wall. Procedia Manufacturing 15: 1232-1238

15. Suzuki, N, Tokuhiro S, Takeuchi O (2018) Double cylinder forming by die-less shear spinning for air intake lip skin of aero jet engine nacelle. Procedia Manufacturing, 15: 1270-1277

16. Qi Zhang, Tong T Zhang, Lei Lei and Min Q Dai (2014) The high-pressure liquid jet incremental forming for the aluminium sheet. Proc IMechE Part B: J Engineering

17. Mao H, He K, Luo Q, Du R (2011) Theoretical and experimental analysis on deformation of sheet metal under waterjet impact loading. Proceeding of the IEEE International Conference on Information and Automation, Shenzhen, China, pp. 295–300

18. Li J, He K, Wei S, Dang X, Du R (2014) Modeling and experimental validation for truncated cone parts forming based on water jet incremental sheet metal forming. Int J Adv Manuf Technol 75(9):1691–1699

19. Shi Y, Cao J, Ehmann K F (2018) Dieless water jet incremental micro-forming. In *International Manufacturing Science and Engineering Conference* (Vol. 51388, p. V004T03A011). American Society of Mechanical Engineers.

20. Shi Y, Zhang W, Cao J, Ehmann K F (2019) An experimental and numerical study of dieless water jet incremental microforming. *Journal of Manufacturing Science and Engineering*, *141*(4).

21. Shi Y, Zhang W, Cao J, Ehmann K. F. (2019). Experimental study of water jet incremental micro-forming with supporting dies. *Journal of Materials Processing Technology*, *268*, 117-131

22. Zhang Q, Zhang T, Dai M, Fan S, Ben N, Wu S (2016) Numerical simulation and experimental research on water jet forming of copper foil. Int J Adv Manuf Technol 85:2265–2276.

23. Lu B, Bazeer M M, Cao J F, Ai S, Chen J, Ou H, Long H (2017) A study of incremental sheet forming by using water jet. Int J Adv Manuf Technol *91*(5): 2291-2301.

Figures

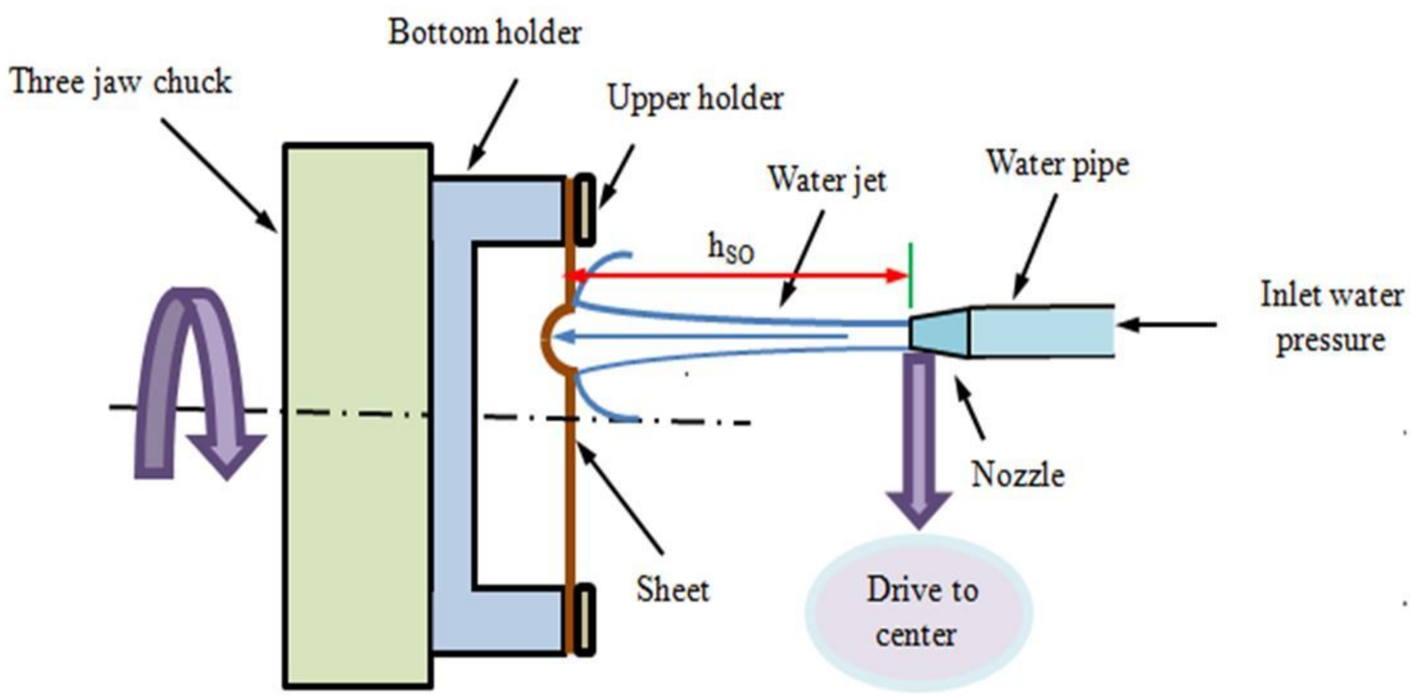

Figure 1

A schematic of die-less water jet spin forming (WJSF).

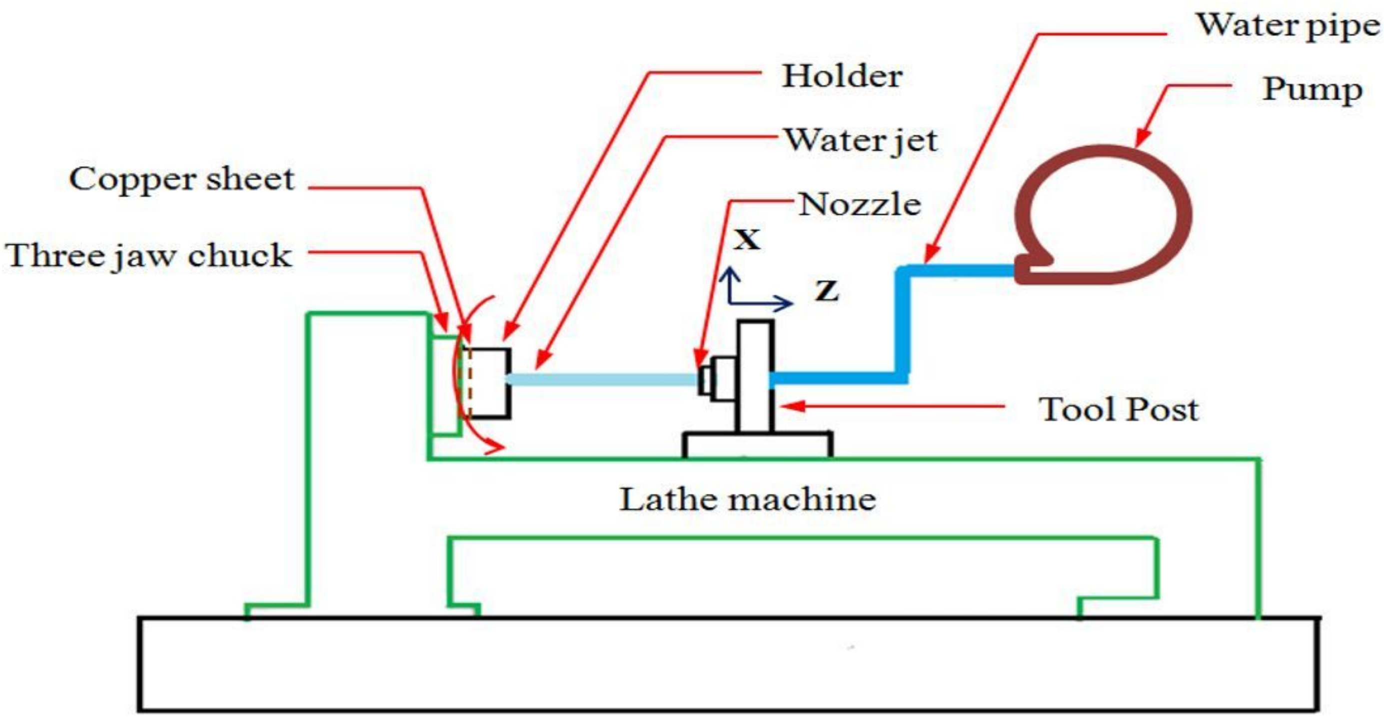

Figure 2

A Schematic of WJSF setup

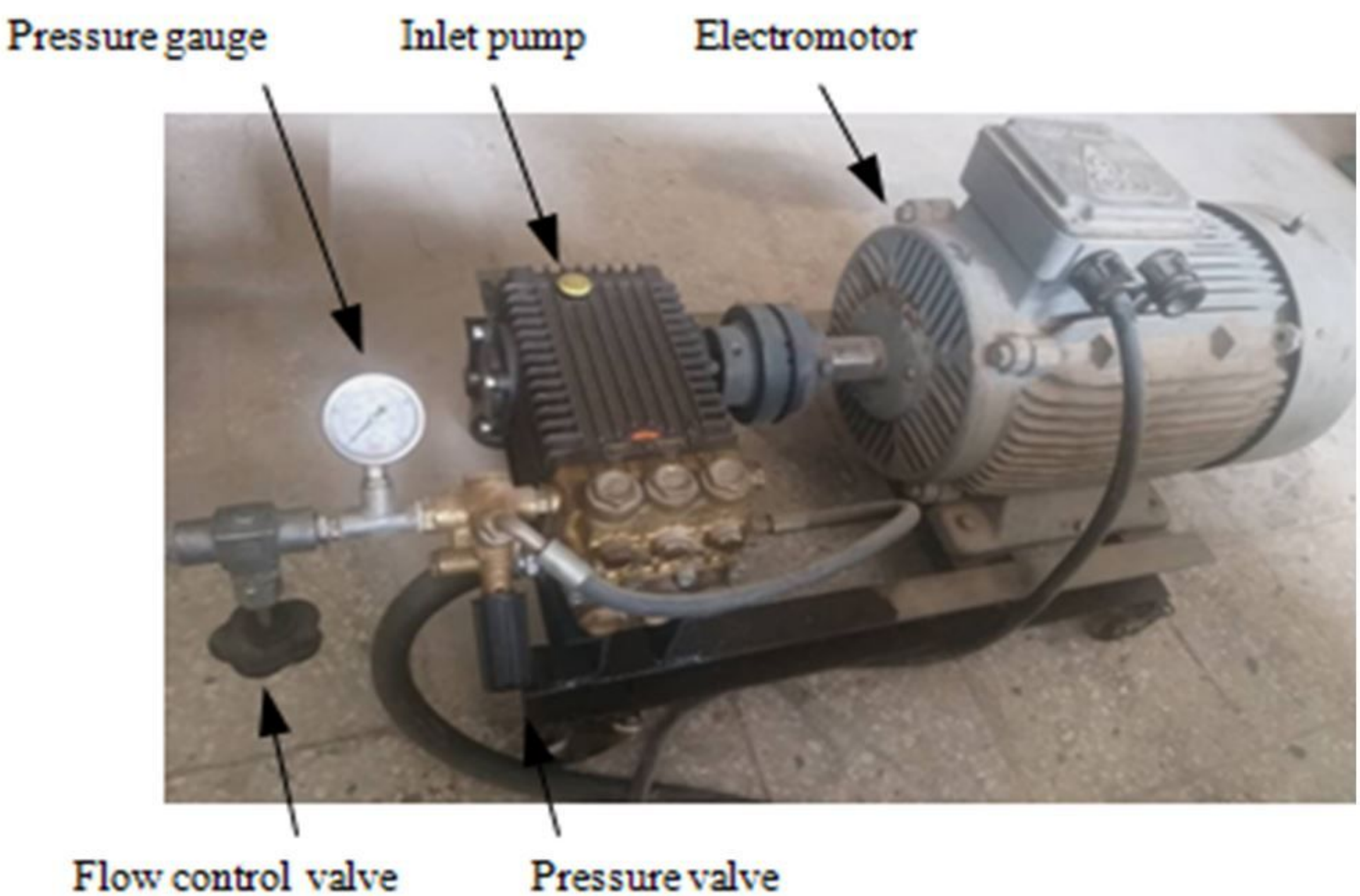

Figure 3

Piston pump and electromotor.

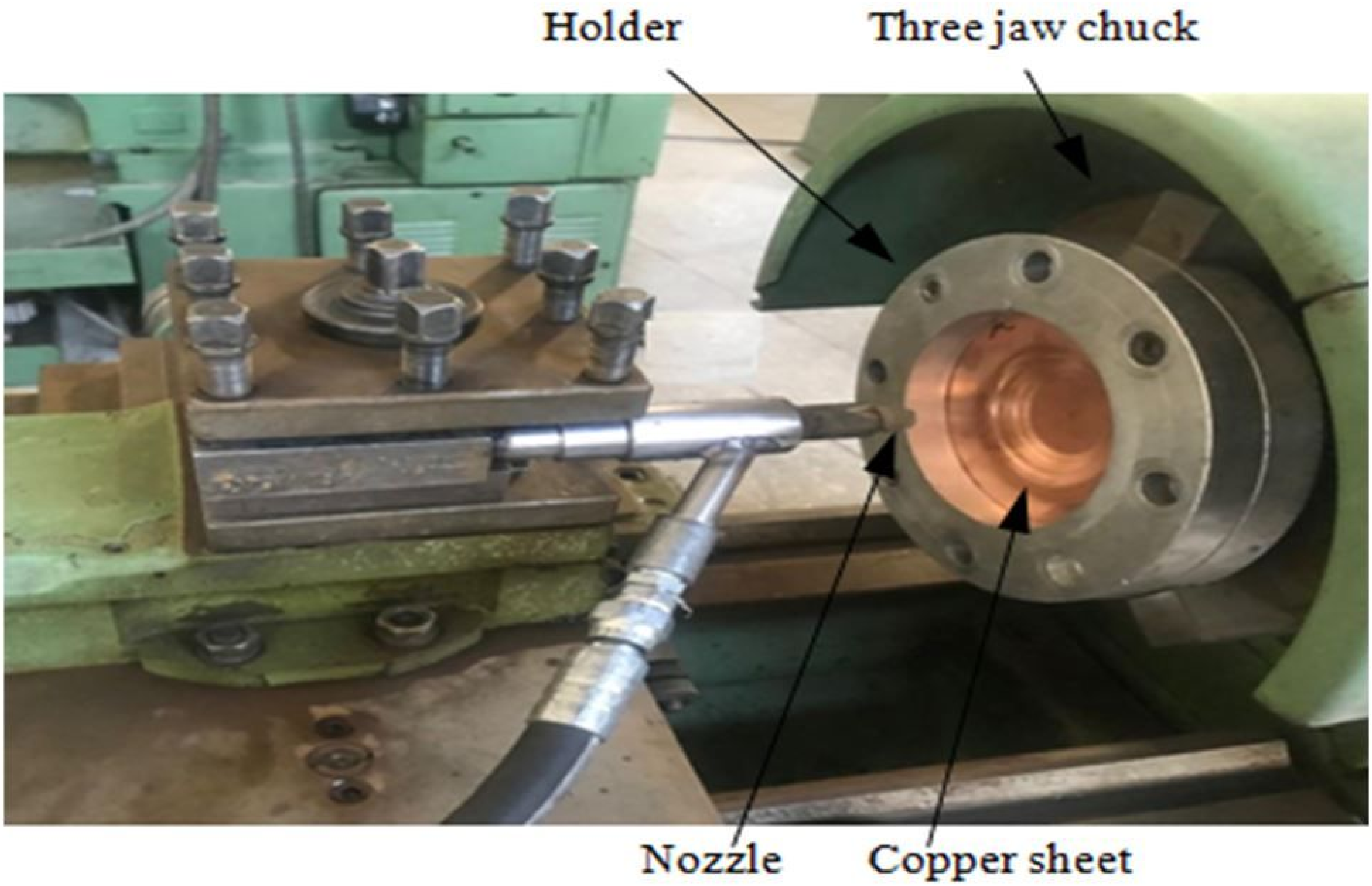

Figure 4

Lathe machine and nozzle used for WJDF process.

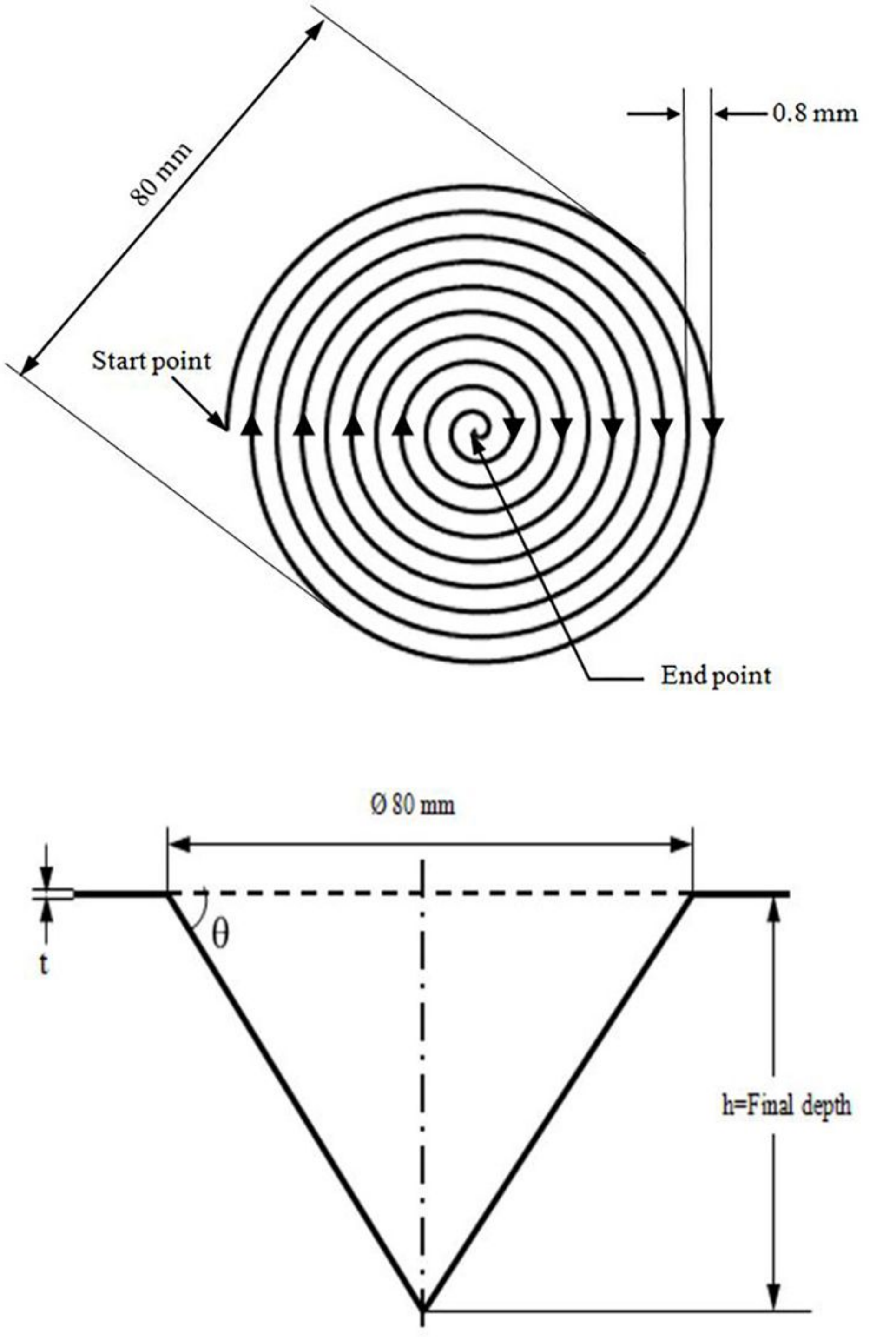

Figure 5

Schematic of spiral path of a water jet and final shape of a complete cone

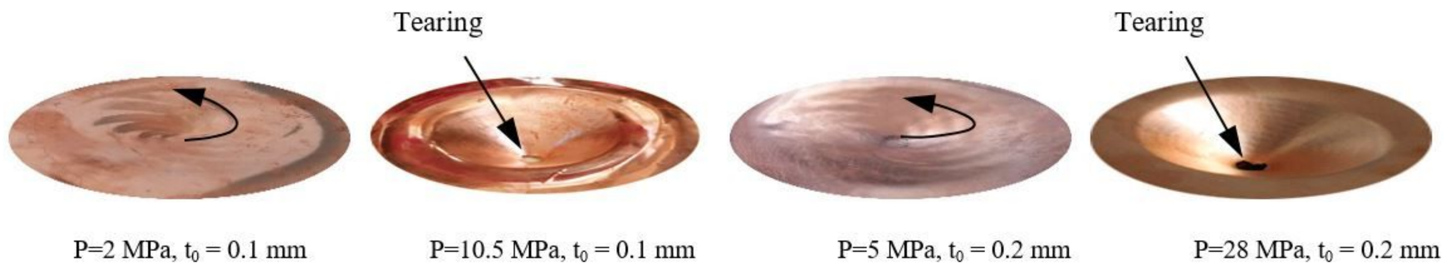

Figure 6

Deformed specimens with yield pressure and final pressure for different thicknesses of copper sheets.

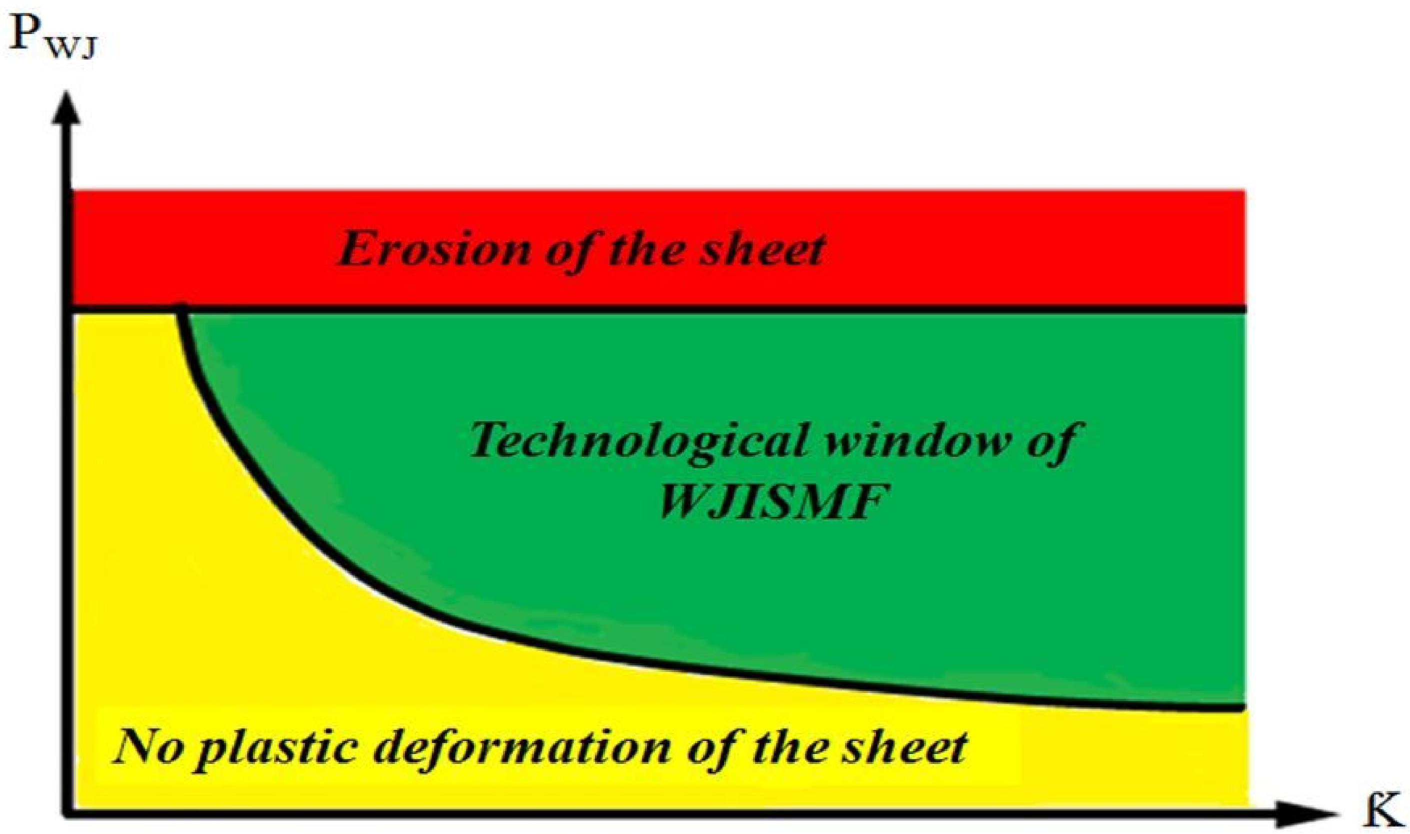

Figure 7

Schematic diagram of Technological window of WJIF process.

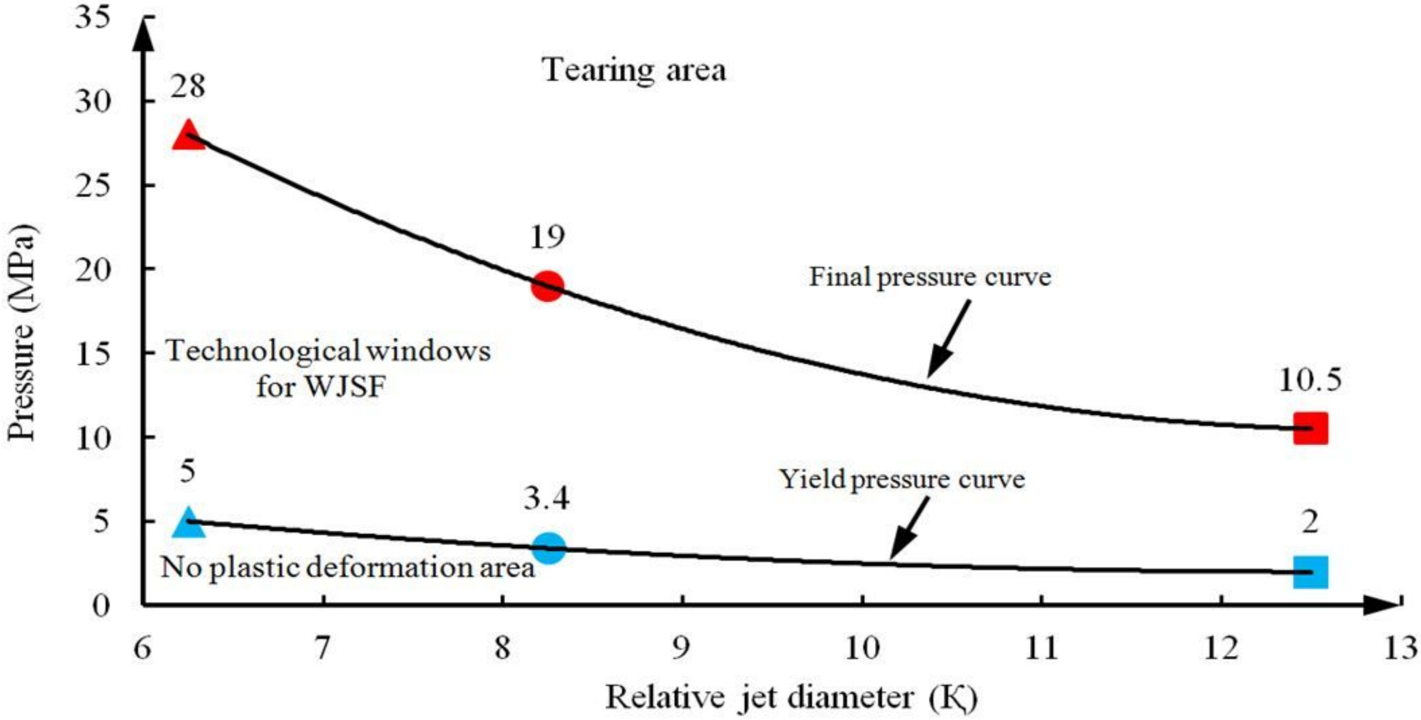

Figure 8

Technological window of WJSF for different sheet thicknesses obtained by experiments.

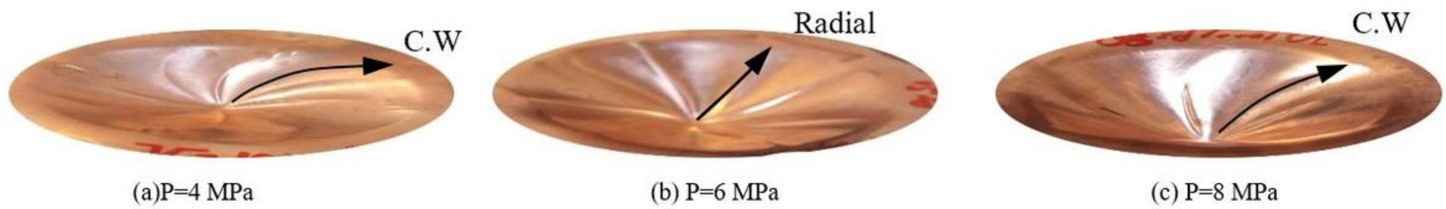

Figure 9

Deformed copper sheets with rotational speeds of 1000 RPM.

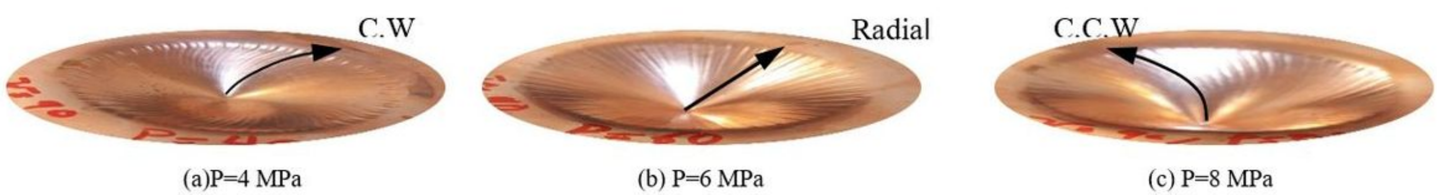

Figure 10

Deformed copper sheets with rotational speeds of 90 RPM.

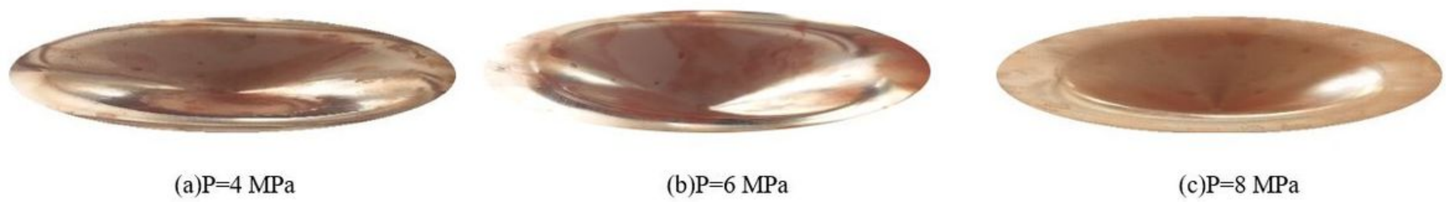

Figure 11

Deformed copper sheets with rotational speeds of 22 RPM.

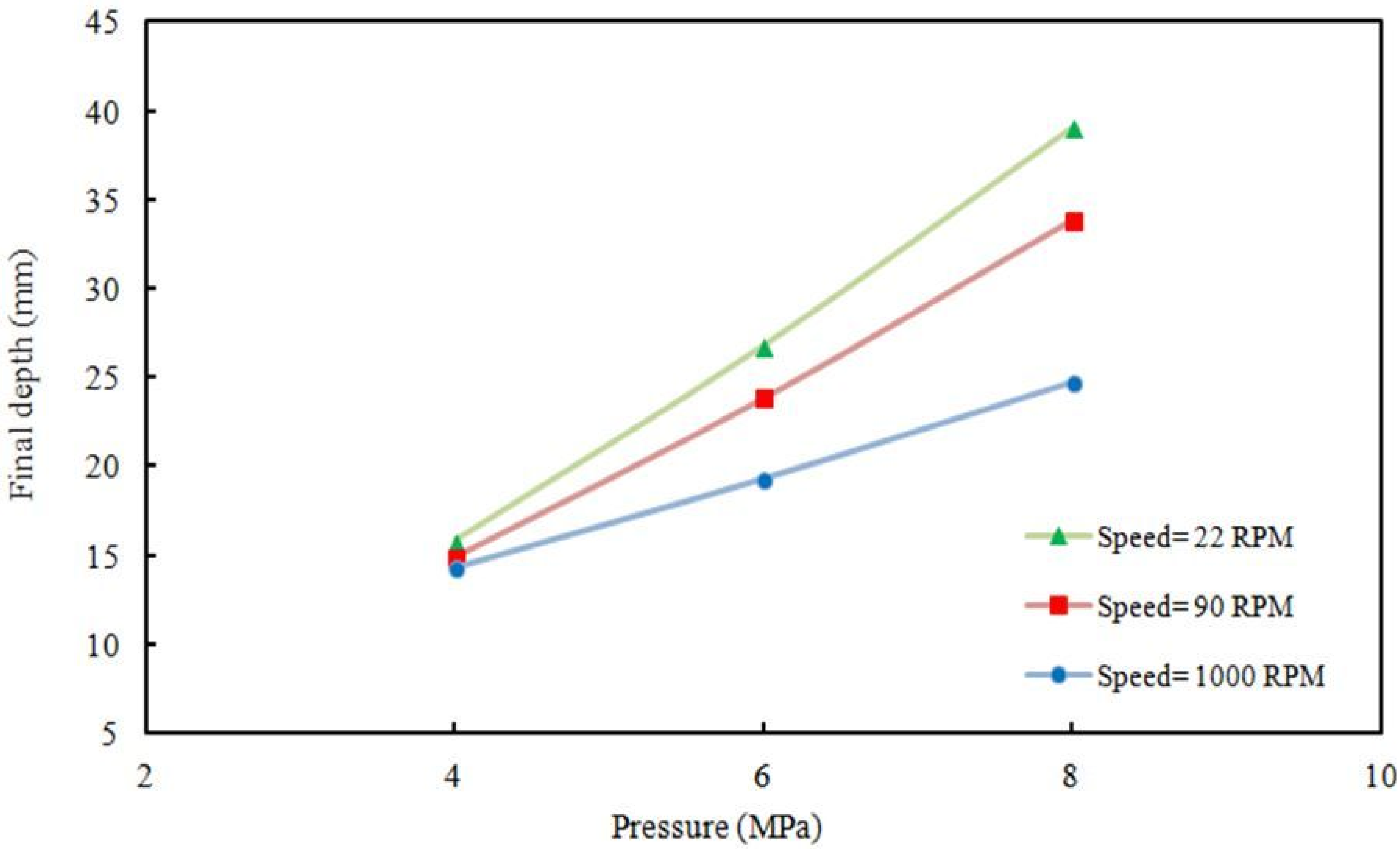

Figure 12

Final depths for different pressures and rotational speeds.

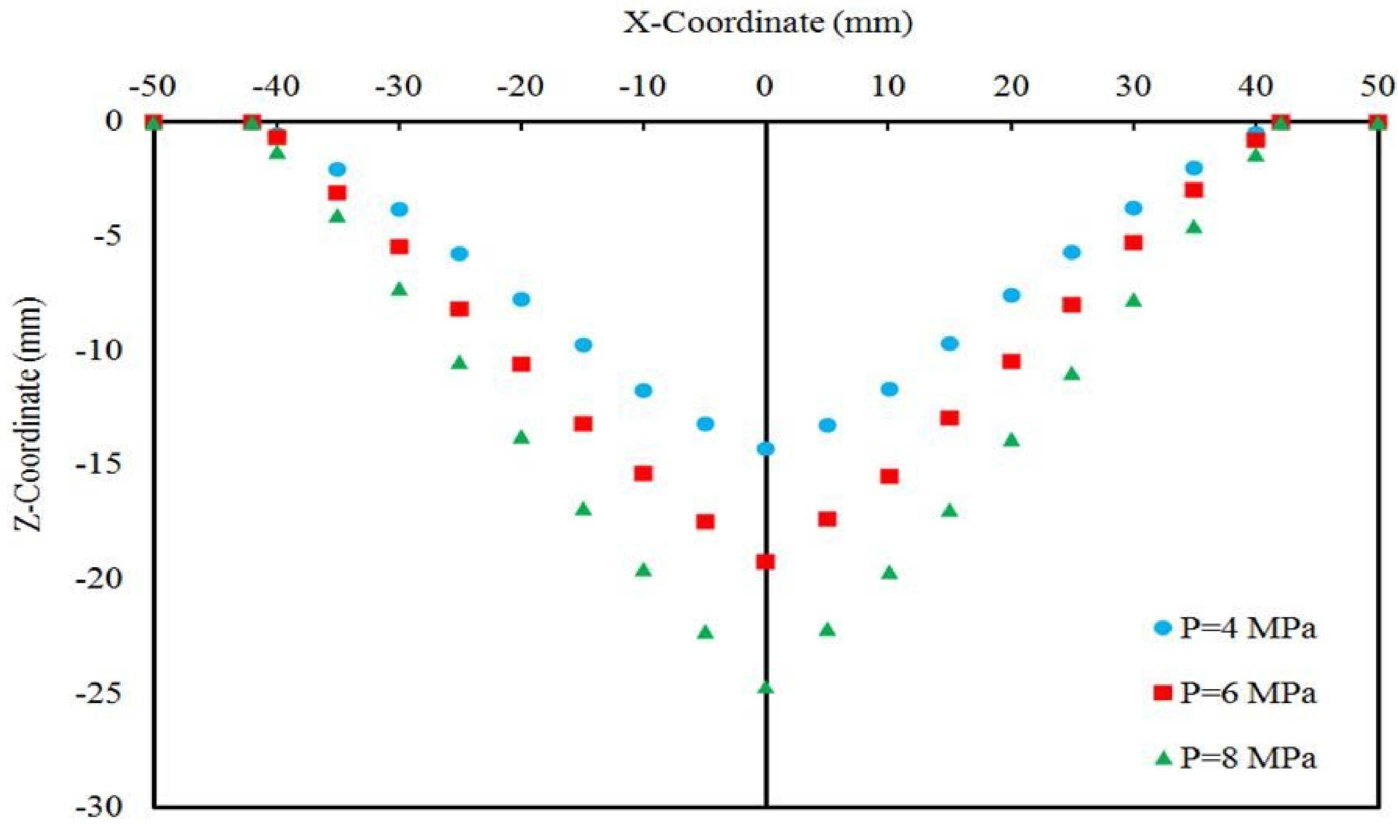

Figure 13

Comparison between cross-sectional shapes of deformed area obtained by different pressure with a rotation speed of 1000 RPM.

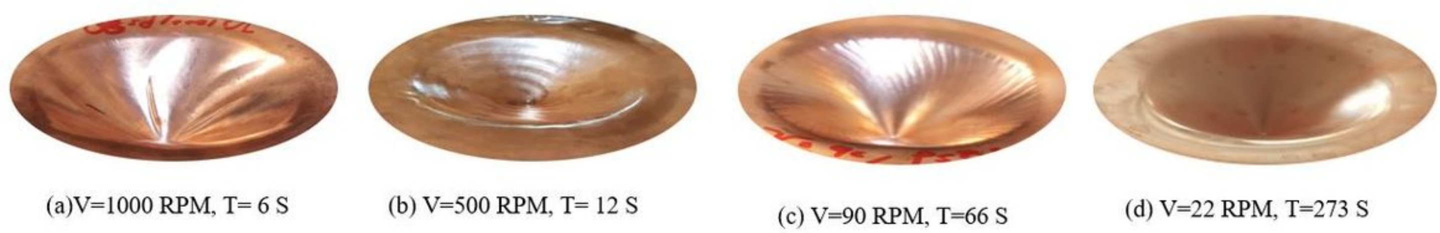

Figure 14

Deformed copper sheets with W pressure of 8 MPa.

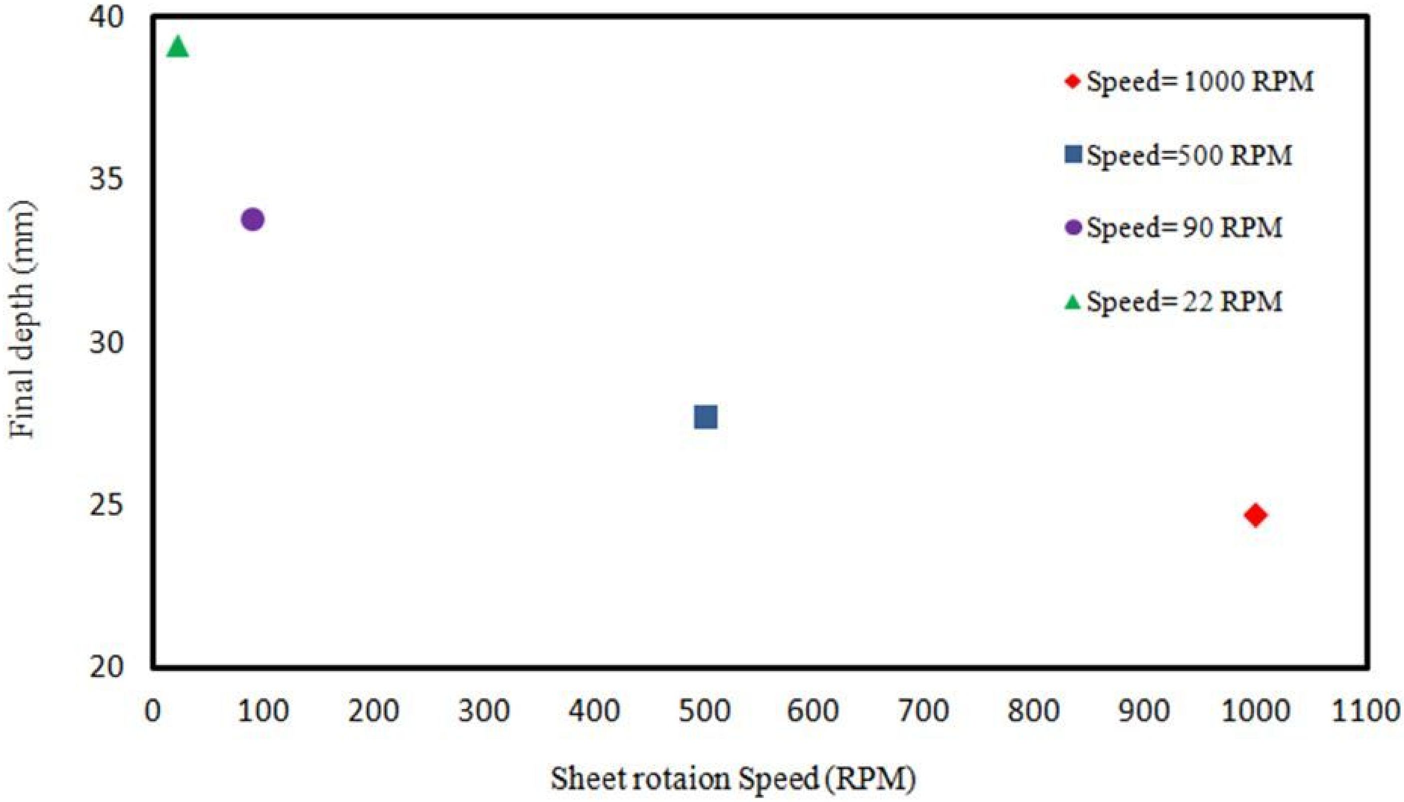

Figure 15

Final depth of deformed parts for different rotational speeds and WJ pressure of 8 MPa.

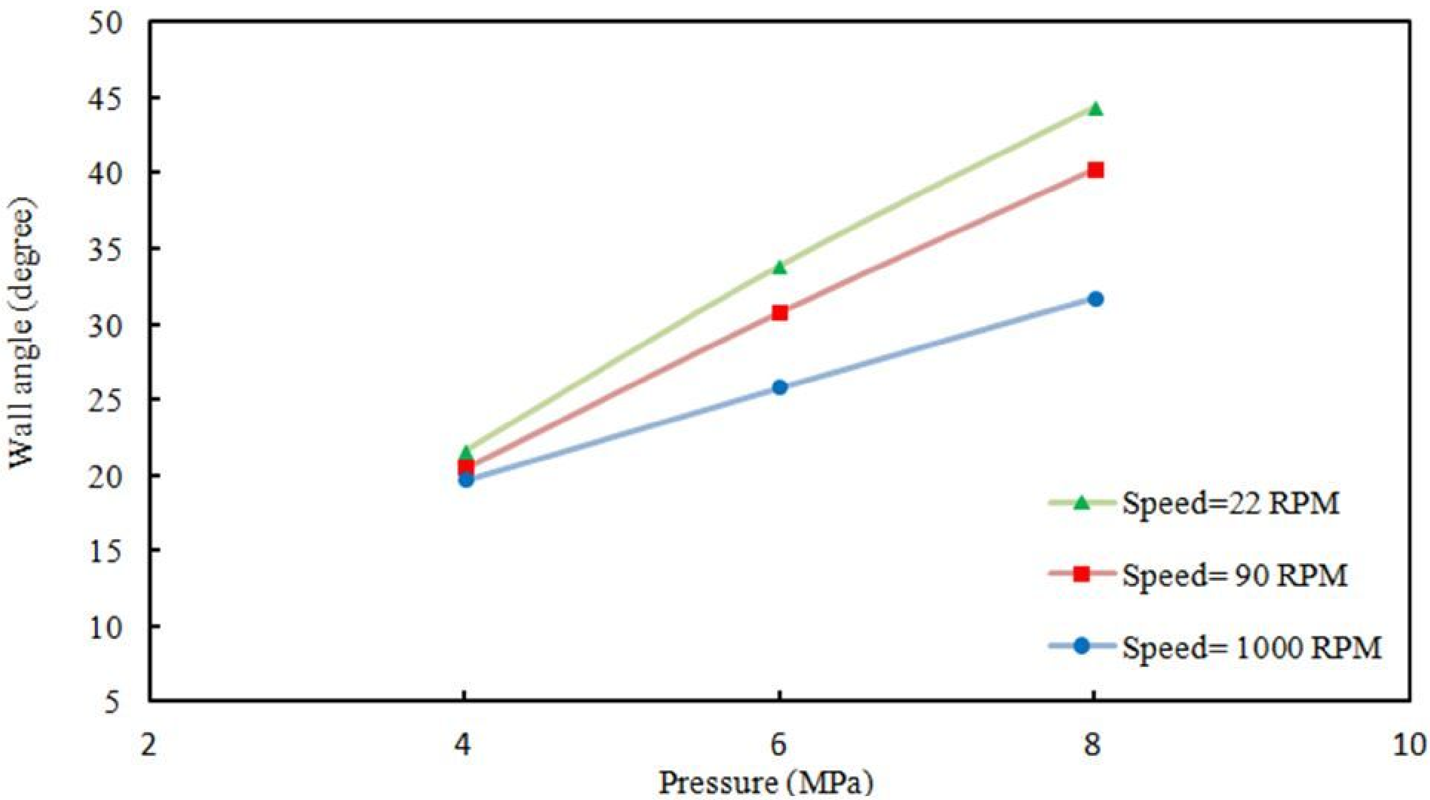

Figure 16

Comparison of wall angles with different pressures and rotational speed of 22, 90, and 1000 RPM.

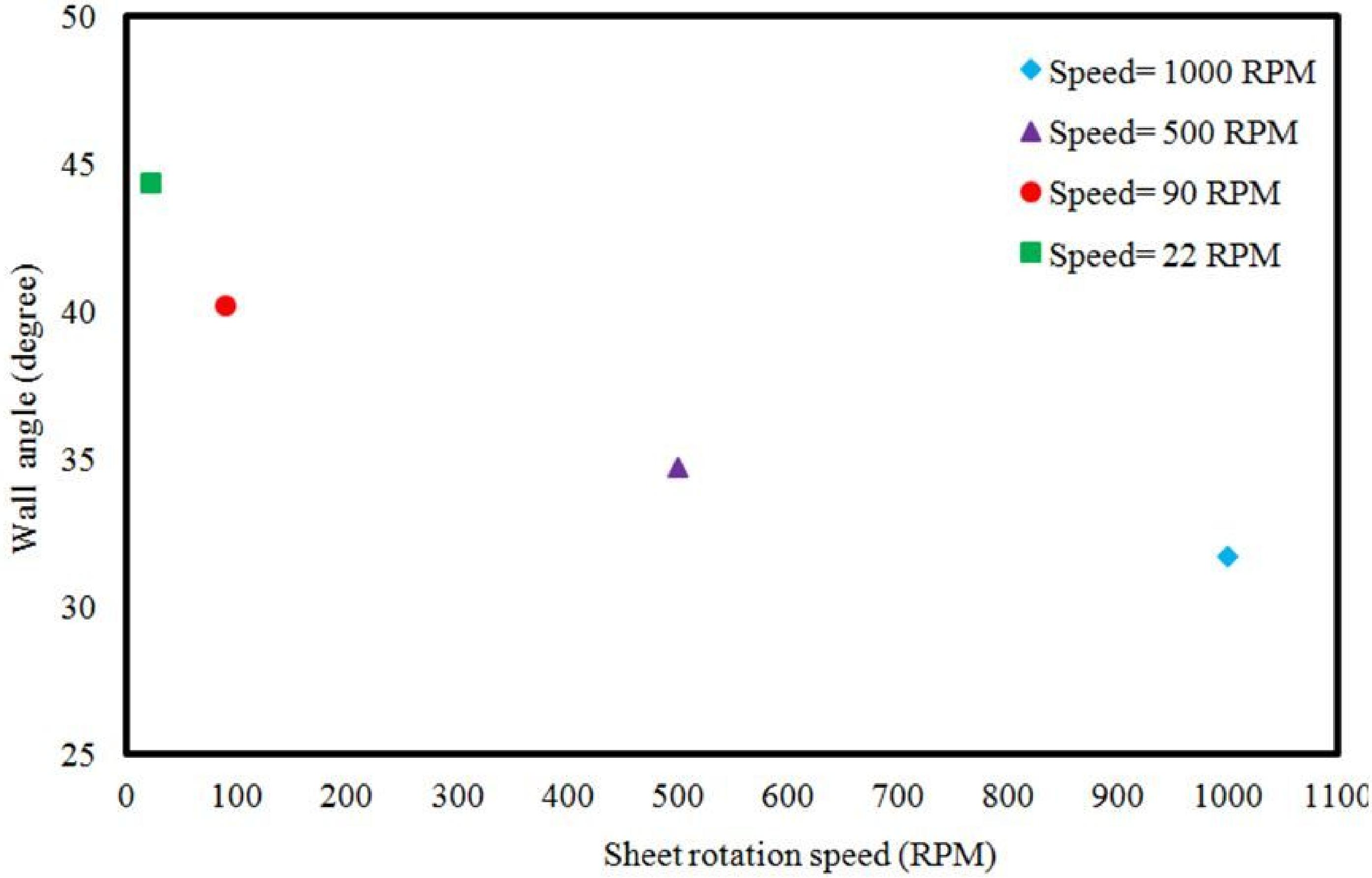

Figure 17

Comparison between wall angles for different rotational speeds and with WJ pressure of 8 MPa.

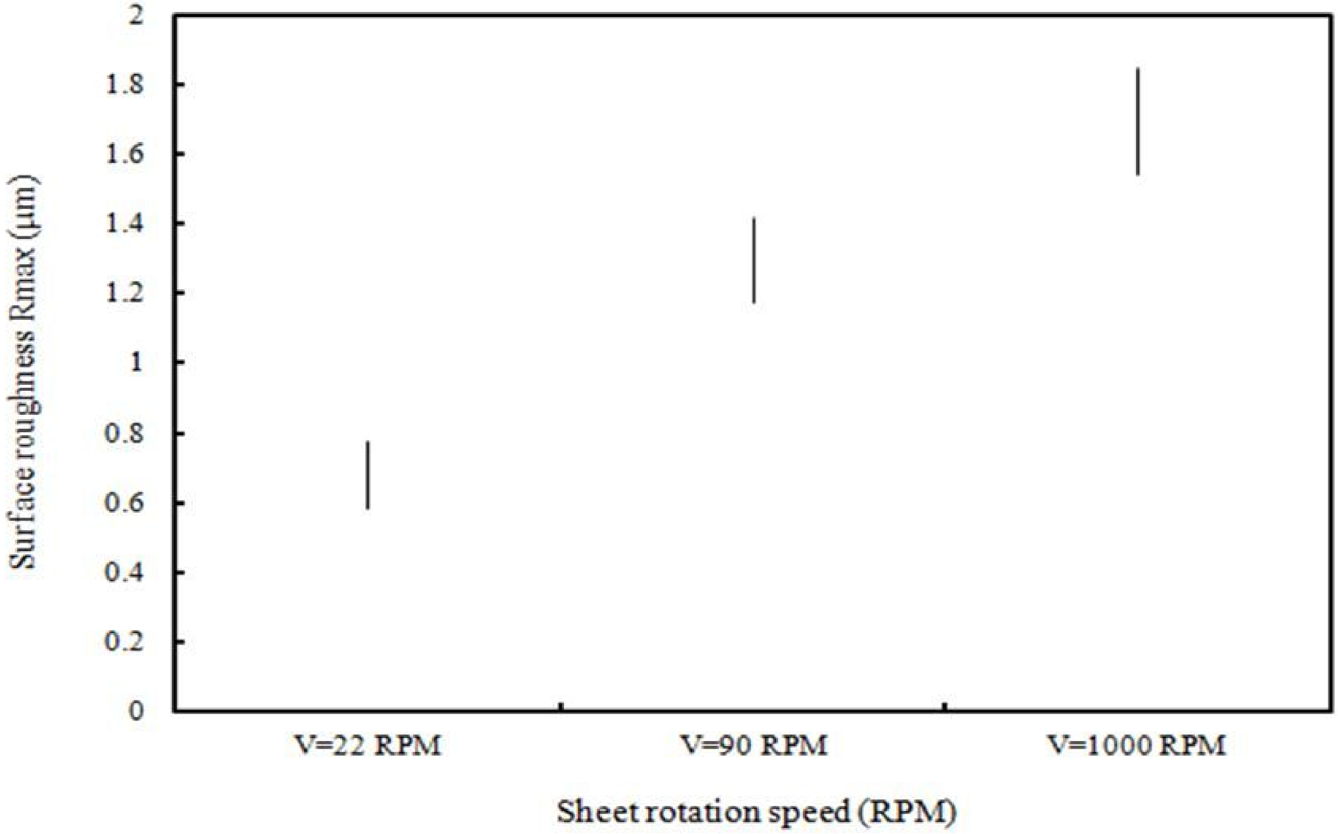

Figure 18

Comparison of surface roughness with different sheet rotation speeds and WJ pressure of 4 MPa.

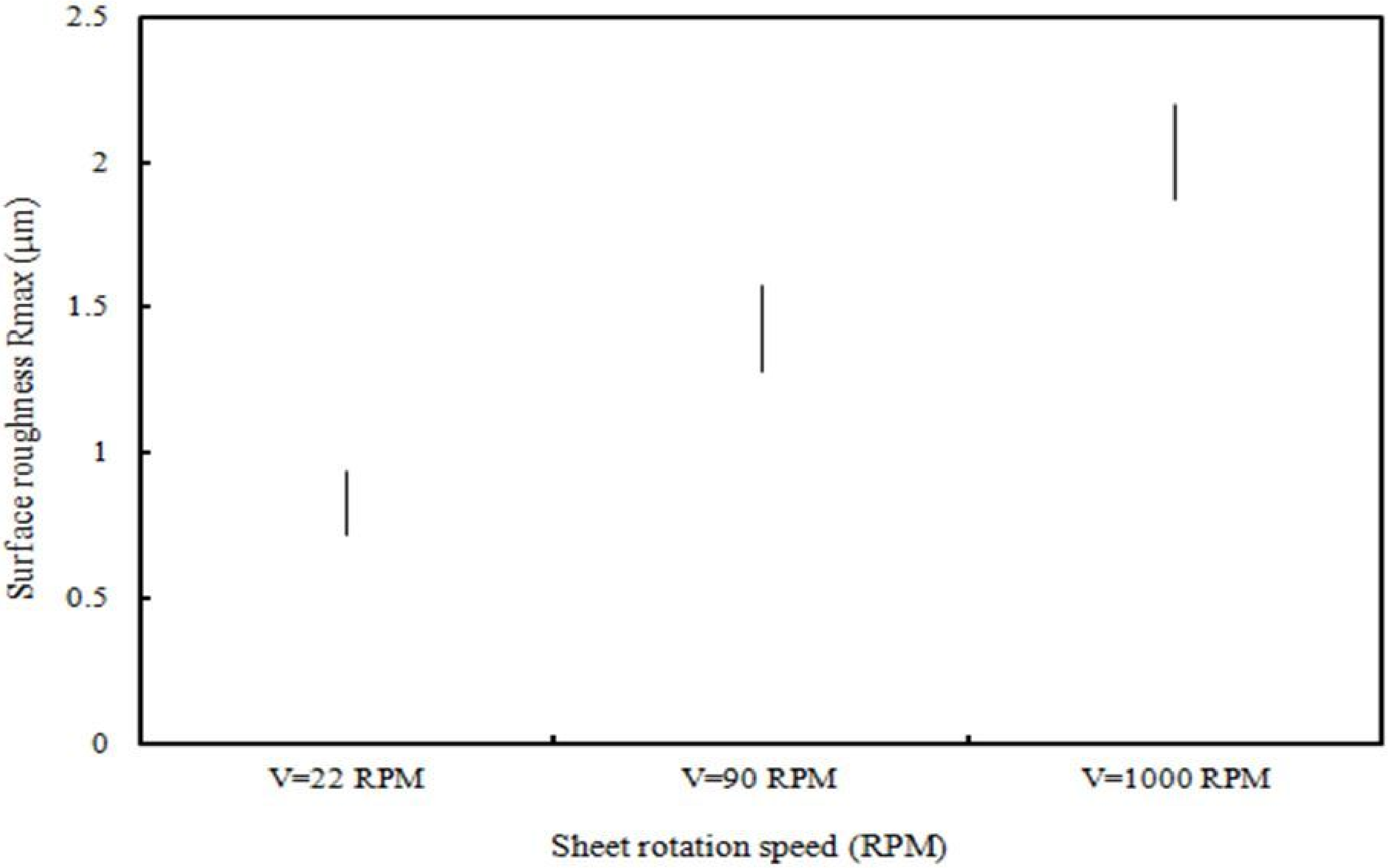

Figure 19

Comparison of surface roughness with different rotational speeds and WJ pressure of 6 MPa.

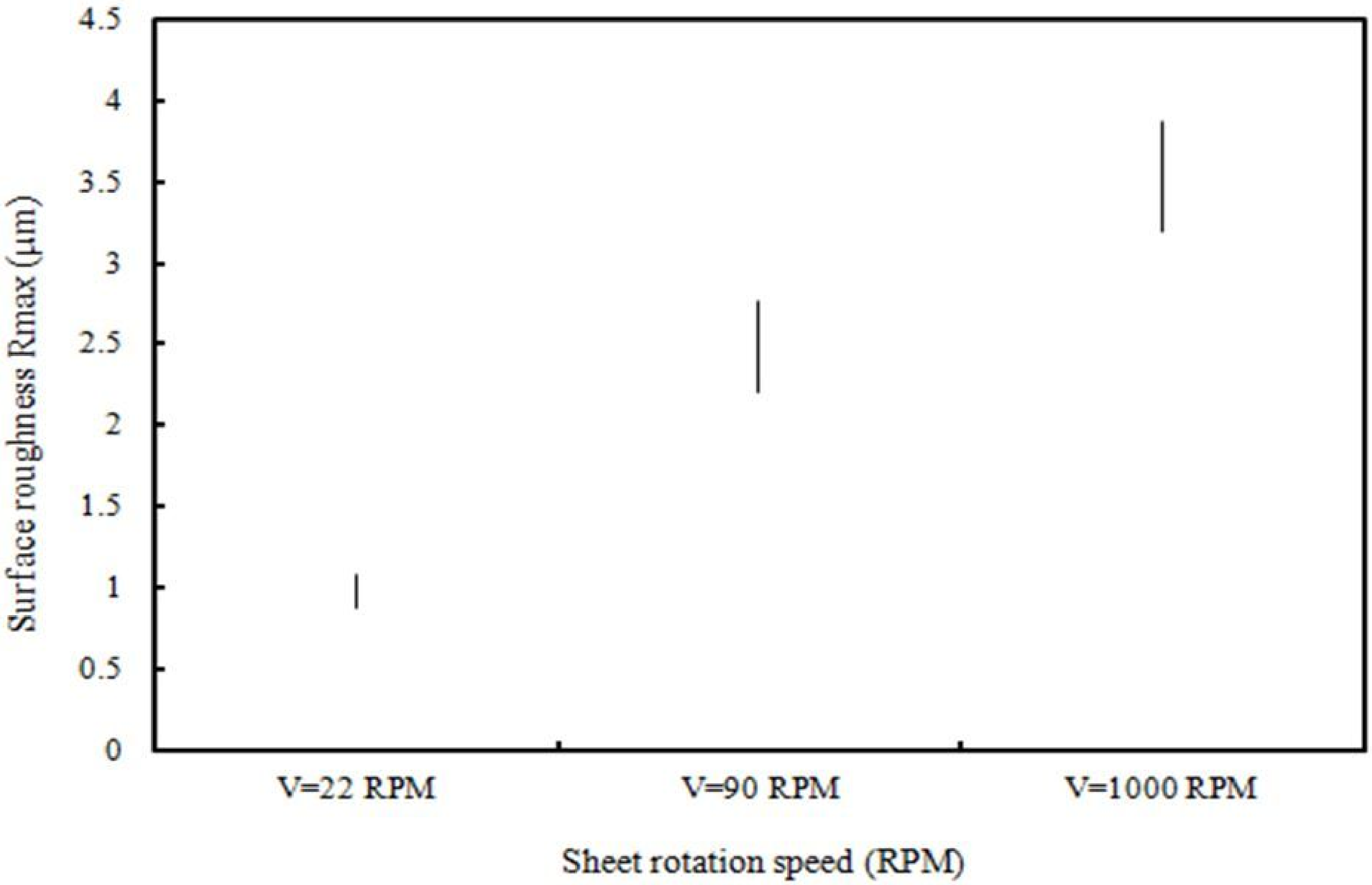

Figure 20

Comparison of surface roughness with different rotational speeds and WJ pressure of 8 MPa.

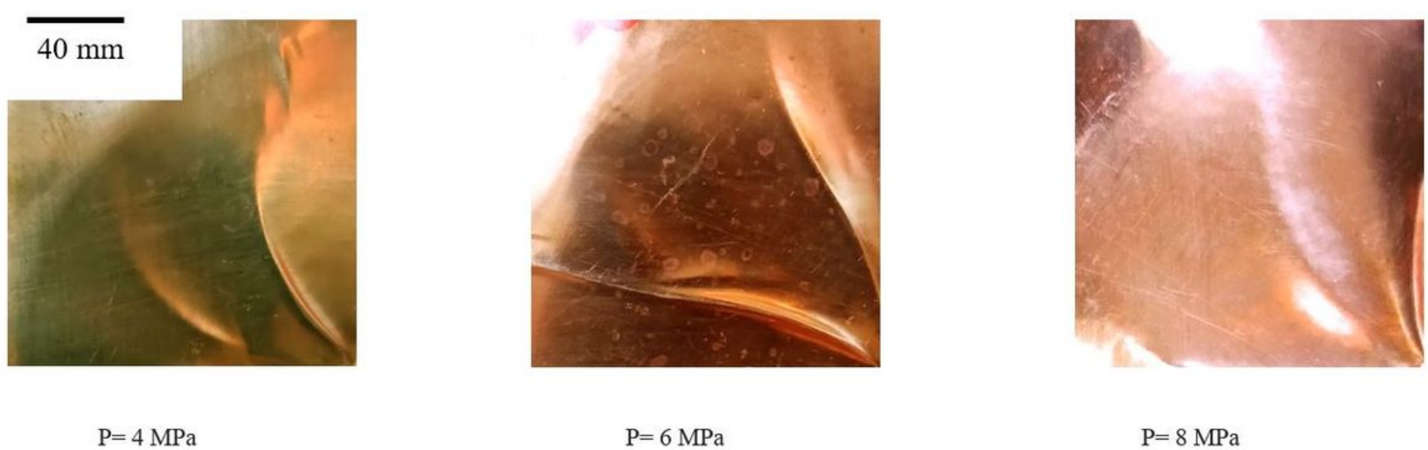

Figure 21

Microscopic images of the deformed surfaces of the cone parts with different pressures and speeds of 1000 RPM.

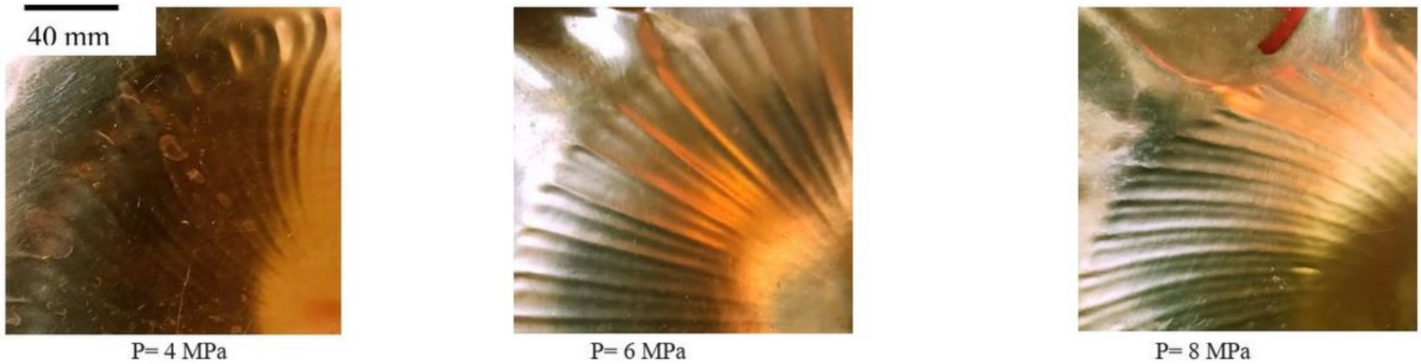

Figure 22

Microscopic images of the deformed surfaces of the cone parts with different pressures and speeds of 90 RPM

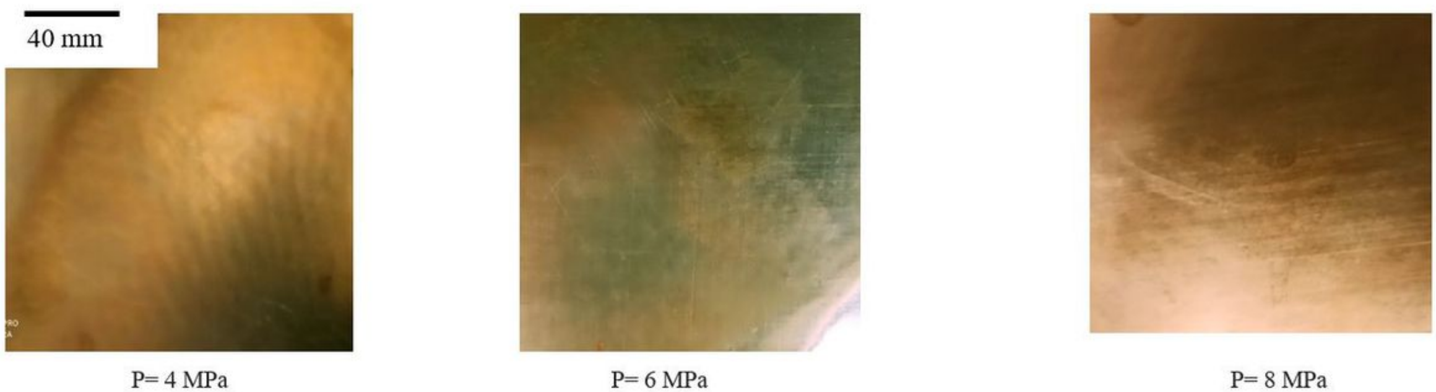

Figure 23

Microscopic images of the deformed surfaces of the cone parts with different pressures and speeds of 22 RPM.

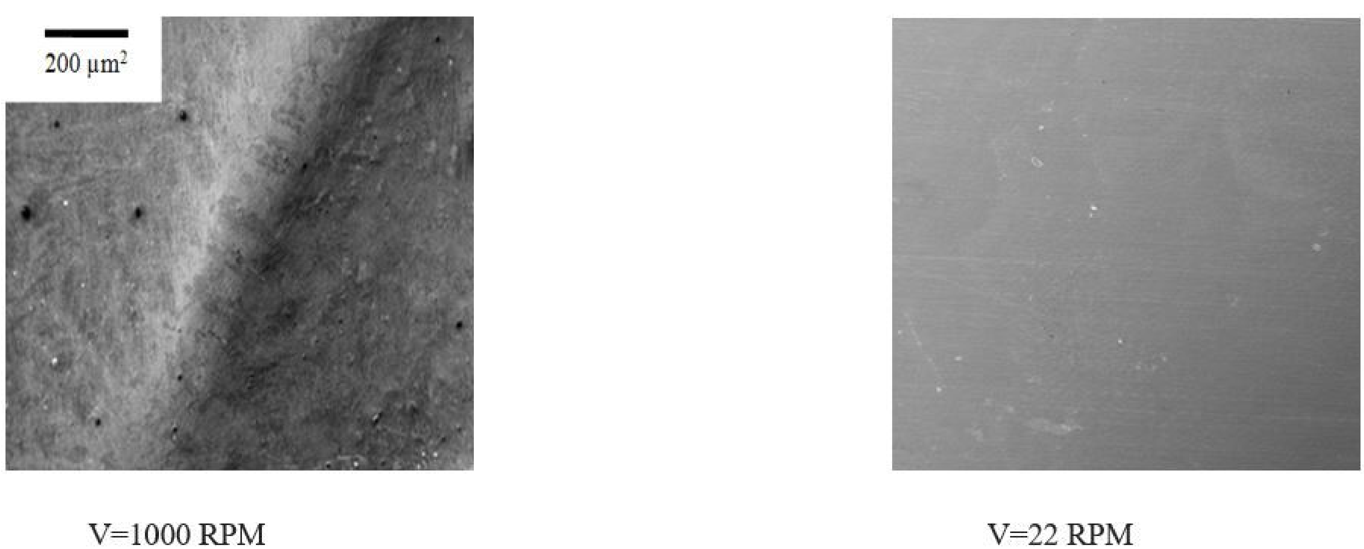

Figure 24

SEM images with 50x magnification, for two formed specimens with speeds of 1000 and 22 RPM and pressure of 4 MPa.